Hindawi Publishing Corporation
Journal of Nanomaterials
Volume 2013, Article ID 909786, 6 pages
http://dx.doi.org/10.1155/2013/909786

Research Article

All-Solution-Processed $InGaO_3(ZnO)_m$ Thin Films with Layered Structure

Sung Woon Cho,[1] Jun Hyeon Kim,[1] Sangwoo Shin,[2] Hyung Hee Cho,[2] and Hyung Koun Cho[1]

[1] *School of Advanced Materials Science and Engineering, Sungkyunkwan University, 2066 Seobu-ro, Jangan-gu, Suwon, Gyeonggi-do 440-746, Republic of Korea*
[2] *Department of Mechanical Engineering, Yonsei University, Seoul 120-749, Republic of Korea*

Correspondence should be addressed to Hyung Koun Cho; chohk@skku.edu

Received 14 June 2013; Revised 29 August 2013; Accepted 29 August 2013

Academic Editor: Chan Park

We fabricated the crystallized InGaZnO thin films by sol-gel process and high-temperature annealing at 900°C. Prior to the deposition of the InGaZnO, ZnO buffer layers were also coated by sol-gel process, which was followed by thermal annealing. After the synthesis and annealing of the InGaZnO, the InGaZnO thin film on the ZnO buffer layer with preferred orientation showed periodic diffraction patterns in the X-ray diffraction, resulting in a superlattice structure. This film consisted of nanosized grains with two phases of $InGaO_3(ZnO)_1$ and $InGaO_3(ZnO)_2$ in InGaZnO polycrystal. On the other hand, the use of no ZnO buffer layer and randomly oriented ZnO buffer induced the absence of the InGaZnO crystal related patterns. This indicated that the ZnO buffer with high *c*-axis preferred orientation reduced the critical temperature for the crystallization of the layered InGaZnO. The InGaZnO thin films formed with nanosized grains of two-phase $InGaO_3(ZnO)_m$ superlattice showed considerably low thermal conductivity (1.14 $Wm^{-1}K^{-1}$ at 325 K) due to the phonon scattering from grain boundaries as well as interfaces in the superlattice grain.

1. Introduction

The complex materials based on PbTe and SiGe have been considered for thermoelectric application due to high ZT values at mid- (500–900 K) and high- (>900 K) temperature range. Recently, it was reported that nanosized inclusions (in bulk system) or nanocomposites (in low-dimensional system) in host material enhance dimensionless thermoelectric figure of merit, $ZT = S^2\sigma T/\kappa$ (S: Seebeck coefficient, σ: electrical conductivity, T: temperature, and κ: thermal conductivity). There are two principle reasons for ZT increase. First, Seebeck coefficient is remarkably increased by energy filtering for electrons or holes with low energy. Second, thermal conductivity is decreased due to more frequent phonon scattering by new generated interfaces, which is the main reason for the dramatic ZT increase [1]. In PbTe based materials, it was proven that nanoinclusions related to Pb, Sb, and Bi decrease thermal conductivity by forming numerous interfaces in PbTe matrix, theoretically [2] and experimentally [3]. In addition, p-type SiGe nanocomposite synthesized by sintering nanopowder also showed a half of thermal conductivity ($\kappa_{\text{nanocomposite}} = \sim 2.3\ Wm^{-1}K^{-1}$ at 1000 K) compared to that ($\kappa_{\text{bulk}} = \sim 4.5\ Wm^{-1}K^{-1}$ at 1000 K) of SiGe bulk due to new generated grain boundaries [4]. The oxide thermoelectric materials such as $Na_{0.75}CoO_2$ [5], $Ca_3Co_4O_9$ [6], and $SrTiO_3$ [7] have been researched for thermoelectric application at high temperature due to high chemical and thermal stability as well as nontoxic elements.

Over the past ten years, there has been a rising amount of interest in fabricating $RAO_3(MO)_m$ (R = In and rare earth elements; A = Ga, In, Al, and Fe; M = Mg, Co, Cu, and Zn;

m = integer) superlattice structures due to their unexpected physical properties by quantum confinement effects [8, 9]. Thus, a multilayered oxide material with long-range periodic atomic arrangement shows exceptional properties, such as high field-effect mobility in thin-film transistors (TFTs) [10], giant magnetoresistance in ferromagnetic materials [11], and extremely high Seebeck coefficient as well as low thermal conductivity in thermoelectric materials [7]. Hosono group first suggested the $InGaO_3(ZnO)_m$ film with multilayered structure on sapphire substrate by reactive solid-phase epitaxy method based on vacuum process [12]. In addition, the InGaZnO TFT using the $InGaO_3(ZnO)_5$ superlattice grown by reactive solid-phase epitaxy as a channel layer exhibited high field-effect mobility (~80 $cm^2\ V^{-1}\ s^{-1}$) [10]. As a similar approach, our group produced the $InGaO_3(ZnO)_m$ superlattice film using advanced process based on solution process for thermoelectric application [13], because Dresselhaus et al. proposed that multilayered structure (superlattice) can remarkably improve thermoelectric properties [1].

In this study, an all-solution process for fabricating InGaZnO superlattice structure was developed based on the chemical reaction of InGaZnO solution and reactive solid phase epitaxy growth proposed by the Hosono group [12]. ZnO films were first deposited on sapphire substrates by sol-gel coating and then annealed at 900°C for 2 hours. Repeated coating processes led to the formation of ZnO thin film preferentially oriented along the c-axis. Then, amorphous InGaZnO was deposited on ZnO buffer by sol-gel coating and annealed at 900°C for 9 hours. This study is the first report on the synthesis of oxide thin films with superlattice structure based on all-solution method.

2. Experiments

The deposition of the ZnO buffer layer and amorphous InGaZnO layer was performed by sol-gel method. Indium nitrate hydrate [$In(NO_3)_3{\cdot}H_2O$, Aldrich], gallium nitrate hydrate [$Ga(NO_3)_3{\cdot}H_2O$, Aldrich], and zinc acetate dehydrate [$Zn(CH_3COO)_2$, Aldrich] were used as the metal precursors, and 2-methoxyethanol (2ME, $C_3H_8O_2$) and monoethanolamine (MEA, C_2H_7NO) were employed as the solvent and stabilizer, respectively. First, ZnO buffer layers were prepared on sapphire substrates by repeated spin coating processes. The solution mixture consisted of zinc acetate dehydrate, 0.2 M 2ME and 0.3 M MEA, and was processed in a glove box under a nitrogen atmosphere (O_2 and H_2O < 10 ppm). After constant magnetic stirring at 400 rpm on a 70°C hot plate for 1 hour, stable ZnO sol was spin-coated on sapphire substrates at 3000 rpm for 30 s and dried at 250°C for 10 min. The coating process was repeated several times to achieve proper thickness, and postannealing was performed at 900°C for 2 hours for the crystallization of the ZnO film. Next, the zinc acetate, indium nitrate, and gallium nitrate were blended at a ratio of 1 : 1 : 1 and spin-coated on the ZnO buffer layer for the formation of the InGaZnO thin films, which was followed by postannealing at 900°C for 9 hours. The overall process for fabricating the InGaZnO thin films is schematically presented in Figure 1. This approach is the same as the one from our previous report [13] except for the synthesis of ZnO seed layer.

Thermogravimetric analysis (TGA) and differential thermal analysis (DTA) were performed at temperatures ranging from room temperature to 400°C with a heating rate of 8°C/min in air for regulating the chemical reaction temperature. The crystal phase of the crystallized InGaZnO thin films was investigated by X-ray diffraction (XRD) and transmission electron microscopy (TEM). The surface morphology of the buffer layers was observed by field-emission scanning electron microscopy (FE-SEM).

3. Results and Discussion

The TG-DTA results of InGaZnO sol are shown in Figure 2. There are two stages that can be seen at 55–110°C and 230–250°C. The first weight loss at 55–110°C indicates that Zn acetate, In nitrate, and Ga nitrate were decomposed and hydrolyzed to Zn–OH, In–OH, and Ga–OH. The second weight loss at 230–250°C indicates dehydroxylation reaction of M–OH to M–O (M = Zn, In, Ga), and most organic products such as 2ME, CH_3COOH, and HNO_3, as well as H_2O, were evaporated. The overall chemical reaction of the metal precursors for the formation of Zn–O, In–O, and Ga–O was explained in previous research [14]. The coating process was established with TG/DTA results, and high-temperature postannealing was performed for crystallization of these films. For the coating of the ZnO buffer layers, different solute concentrations and repetitions were used to induce different surface morphologies and to achieve proper buffer thicknesses, respectively. As shown in Figure 3(a), the solute concentration of 0.5 M with 2 coatings induced a rough surface with island shape, due to inhomogeneous Zn–O distribution coming from excessive solvent concentration. On the other hand, the solute concentration of 0.2 M with 5 coatings led to a homogeneous and flat surface (Figure 3(b)), after post annealing at 900°C for 2 hours similar to previous research [15]. In addition, the flat surface of the ZnO buffer layer was closely related to the strong c-axis preferred orientation. A more intense ZnO (0002) diffraction peak was observed in the InGaZnO thin film/flat ZnO buffer structure than in the InGaZnO thin film/rough ZnO buffer structure, as shown in Figures 4(b) and 4(c).

Through the solution-based synthesis of the ZnO and InGaZnO and thermal annealing, the crystallized InGaZnO thin films were grown on sapphire substrates with the help of the ZnO buffer layer with high c-axis preferred orientation. Figure 4 shows XRD patterns of InGaZnO thin films before and after annealing at 900°C for 9 hours on different ZnO buffer layers, where the InGaZnO thin film without ZnO buffer was used for comparison. In our study, the ZnO layer oriented along the c-axis acts as a seed layer for the enhanced crystallization of the InGaZnO thin films and finally disappears due to the complete intermixing of the ZnO and InGaZnO layers. The intermixing can be confirmed by no sign of the ZnO diffraction peaks after thermal annealing, as shown in Figures 4(e) and 4(f). As confirmed in Figures 4(a)

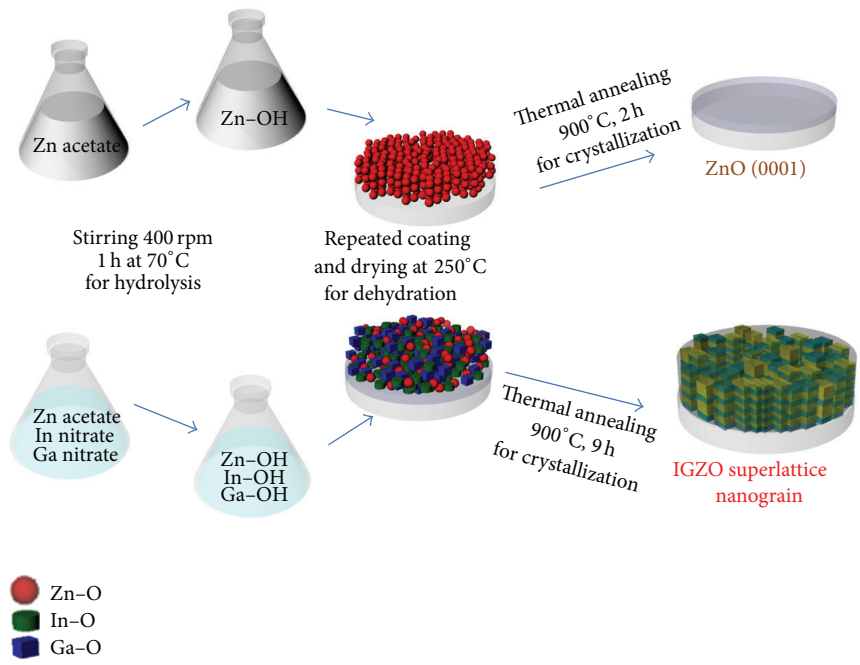

FIGURE 1: The overall fabrication process of the crystallized InGaZnO thin films with nanosize $InGaO_3(ZnO)_m$ superlattice grains, which consisted of sol preparation, spin coating, and thermal annealing.

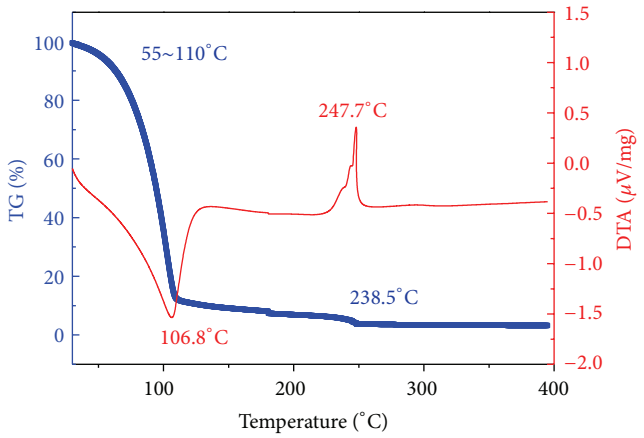

FIGURE 2: Thermogravimetric analysis and differential thermal analysis curves of the InGaZnO sol.

and 4(d), the sample without ZnO buffer shows faint crystallized diffraction patterns that are indexed as GaO, GaZnO, and so forth and are not related to any InGaZnO crystals. This indicates that higher annealing temperature is required for the crystallization of the InGaZnO thin film. Also, a similar result was observed in the sample with rough ZnO buffer layer (or less *c*-axis preferred orientation), as shown in Figure 4(e). However, it is noticeable that many InGaZnO-phases-related peaks were observed from the InGaZnO thin film on the ZnO buffer layer with strong *c*-axis preferred orientation, as shown in Figure 4(f). From the XRD data and JCPS cards (nos. 38-1104 and 40-0252), the 2Θ peaks at 10.2, 20.4, and 30.9° correspond to the (0003), (0006), and (0009) planes of the $InGaO_3(ZnO)_1$ crystal phase, respectively, and the 2Θ peaks at 15.8, 23.8, and 31.9° are in accordance with the (0004), (0006), and (0008) planes of the $InGaO_3(ZnO)_2$ crystal phase, respectively. This result indicates that the ZnO buffer layer with *c*-axis preferred orientation promotes the crystallization of the InGaZnO thin films, and significantly reduces the crystallization temperature [16].

Figures 5(a)–5(c) show cross-sectional bright-field (BF) TEM image, selective area diffraction pattern (SADP), and high-resolution transmission electron microscopy image obtained from InGaZnO thin film using ZnO buffer layer with strong c-axis preferred orientation, respectively. The cross-sectional BF TEM image revealed that the InGaZnO film consists of nano-size grains with the dimension of 100~150 nm, and the film is polycrystal. The nano-size grains have the width of ~150 nm and the height of ~100 nm. As shown in Figures 5(b) and 5(c), SADP and HRTEM image show the existence of $InGaO_3(ZnO)_m$ superlattice along the vertical direction, which is equivalent with XRD data. One nanograin in the bottom region of cross-sectional HRTEM image certainly shows $InGaO_3(ZnO)_m$ superlattice in polycrystalline InGaZnO film.

We had already proven the effectiveness of the $InGaO_3(ZnO)_m$ superlattice structure for improved thermoelectric properties [17], which was attributed to frequent phonon scattering at the interface of InO_2^- and $GaO(ZnO)_m^+$ layer. In this survey, InGaZnO thin film fabricated by all-solution process is polycrystalline with nano-size grains of two-phase $InGaO_3(ZnO)_m$ superlattice, which is expected to induce low thermal conductivity due to

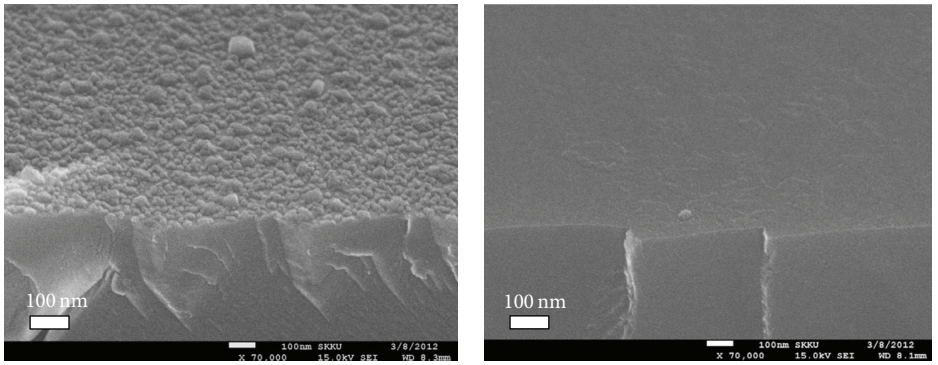

Figure 3: FE-SEM images of ZnO buffer layers with different coating conditions after annealing at 900°C for 2 hours; (a) 0.5 M, 2-time coated ZnO layer and (b) 0.2 M, 5-time coated ZnO layer.

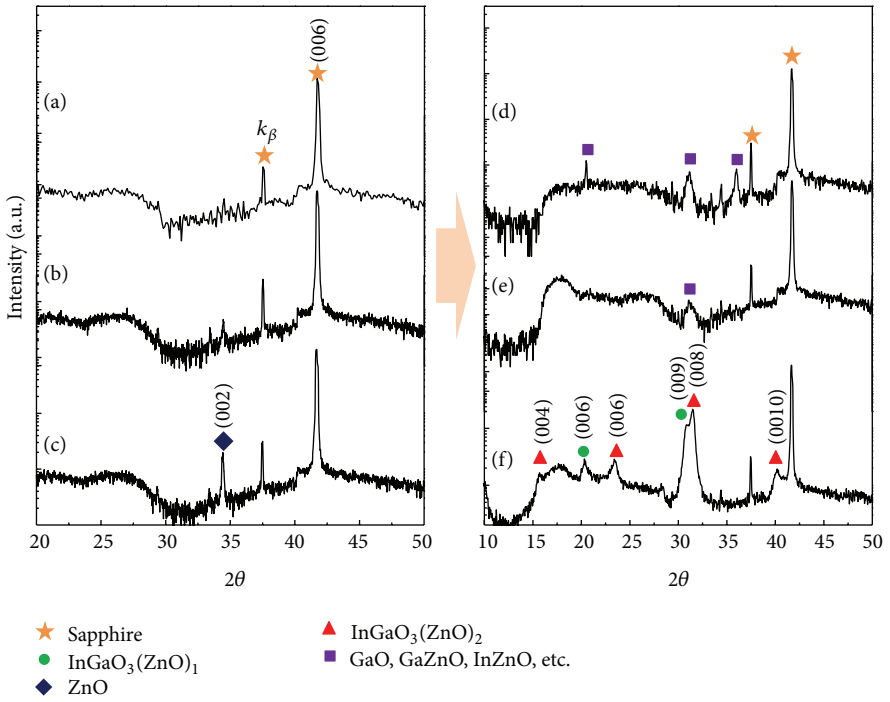

Figure 4: XRD patterns of InGaZnO thin films (a)–(c) before and (d)–(f) after annealing on different buffer layers. (a) and (d) without ZnO buffer, (b) and (e) randomly oriented ZnO buffer layer, and (c) and (f) preferentially oriented ZnO buffer layer.

frequent phonon scattering at the surface of nanograins as well as many interfaces in each $InGaO_3(ZnO)_m$ superlattice nanograin, as shown in Figure 5(d). In previous report by Seo et al. [17], the polycrystalline InGaZnO thin film fabricated by sputtering exhibited high thermal conductivity (7.53 $Wm^{-1}K^{-1}$ at 300 K). In addition, thermal conductivities of ZnO-based materials were also quite high (2~10 $Wm^{-1}K^{-1}$) [18–20]. On the contrary, the polycrystalline InGaZnO thin film with superlattice nanograins fabricated by all-solution process showed considerably low thermal conductivity (1.14 $Wm^{-1}K^{-1}$ at 325 K and 0.99 $Wm^{-1}K^{-1}$ at 355 K).

4. Conclusions

Semiconducting ZnO-based oxide thin films had been developed for various electronic and optoelectronic applications such as transparent TFTs, optical and chemical sensors, and thermoelectrics. These applications can be improved by using layered structures as an active layer. In this study, InGaZnO thin films were fabricated by an all-solution process. Unlike the single phase $InGaO_3(ZnO)_m$ observed in InGaZnO thin film using a epitaxial ZnO buffer grown by vacuum deposition process, the solution-processed ZnO buffer layer with preferred orientation along the *c*-axis resulted in polycrystalline InGaZnO

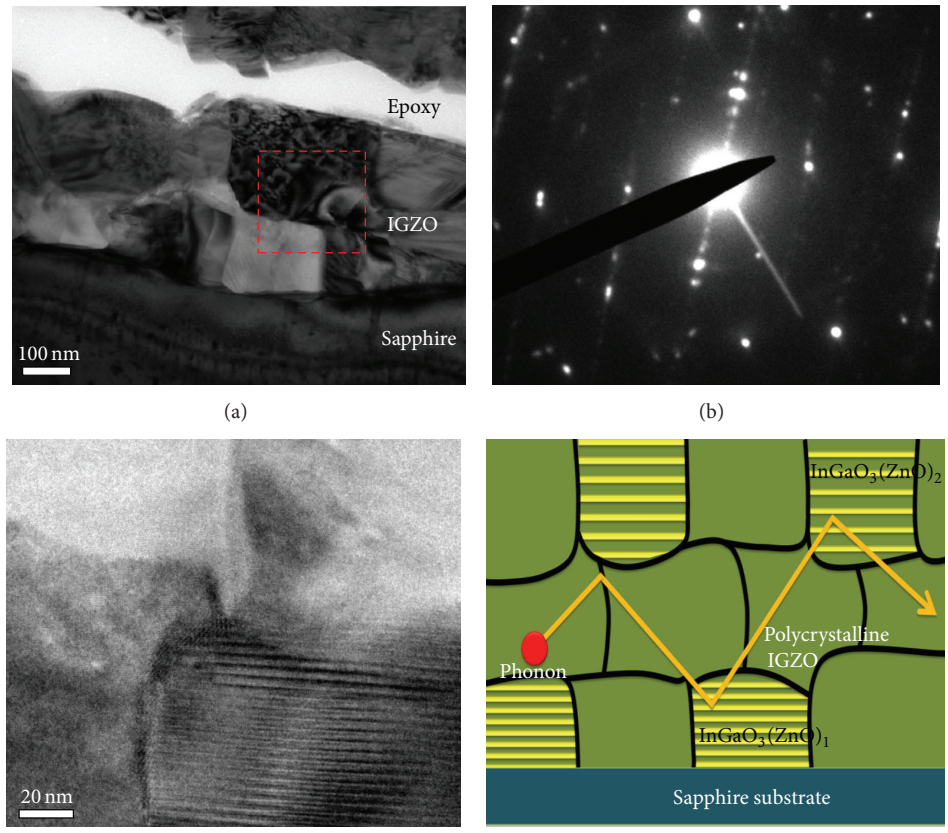

FIGURE 5: (a) Cross-sectional bright-field TEM image, (b) selective area diffraction pattern (SADP) and (c) HRTEM image obtained from $InGaO_3(ZnO)_m$ thin film on ZnO buffer layer with strong *c*-axis preferred orientation. (d) Frequent phonon scattering at the surface of nano-grains as well as the interfaces of the $InGaO_3(ZnO)_m$ superlattice.

film formed with the crystal grains of two phases, such as $InGaO_3(ZnO)_1$ and $InGaO_3(ZnO)_2$. We also obtained extremely low thermal conductivity (1.14 Wm^{-1} K^{-1} at 325 K). This was due to frequent phonon scattering at the surface of nanograins as well as the interfaces of the $InGaO_3(ZnO)_m$ superlattice.

Authors' Contribution

Sung Woon Cho and Jun Hyeon Kim contributed equally to this work.

Acknowledgments

This research was supported by the Basic Science Research Program (2012-0001447) and the Mid-Career Researcher Program (Grant no. 2012-003849) through the National Research Foundation of Korea (NRF) funded by the Ministry of Education, Science and Technology.

References

[1] M. S. Dresselhaus, G. Chen, M. Y. Tang et al., "New directions for low-dimensional thermoelectric materials," *Advanced Materials*, vol. 19, no. 8, pp. 1043–1053, 2007.

[2] S. V. Faleev and F. Léonard, "Theory of enhancement of thermoelectric properties of materials with nanoinclusions," *Physical Review B*, vol. 77, no. 21, Article ID 214304, 2008.

[3] J. He, J. R. Sootsman, S. N. Girard et al., "On the origin of increased phonon scattering in nanostructured pbte based thermoelectric materials," *Journal of the American Chemical Society*, vol. 132, no. 25, pp. 8669–8675, 2010.

[4] G. Joshi, H. Lee, Y. Lan et al., "Enhanced thermoelectric figure-of-merit in nanostructured p-type silicon germanium bulk alloys," *Nano Letters*, vol. 8, no. 12, pp. 4670–4674, 2008.

[5] I. Terasaki, Y. Sasago, and K. Uchinokura, "Large thermoelectric power in $NaCo_2O_4$ single crystals," *Physical Review B*, vol. 56, no. 20, pp. R12685–R12687, 1997.

[6] M. Shikano and R. Funahashi, "Electrical and thermal properties of single-crystalline $(Ca_2CoO_3)_{0.7}CoO_2$ with a $Ca_3Co_4O_9$ structure," *Applied Physics Letters*, vol. 82, no. 12, pp. 1851–1853, 2003.

[7] H. Ohta, S. Kim, Y. Mune et al., "Giant thermoelectric Seebeck coefficient of a two-dimensional electron gas in $SrTiO_3$," *Nature Materials*, vol. 6, no. 2, pp. 129–134, 2007.

[8] H. Hiramatsu, W. S. Seo, and K. Koumoto, "Electrical and optical properties of radio-frequency-sputtered thin films of $(ZnO)_5In_2O_3$," *Chemistry of Materials*, vol. 10, no. 10, pp. 3033–3039, 1998.

[9] J. L. F. Da Silva, Y. Yan, and S. H. Wei, "Rules of structure formation for the homologous $InMO_3(ZnO)_n$ compounds," *Physical Review Letters*, vol. 100, no. 25, Article ID 255501, 2008.

[10] K. Nomura, H. Ohta, K. Ueda, T. Kamiya, M. Hirano, and H. Hosono, "Thin-film transistor fabricated in single-crystalline transparent oxide semiconductor," *Science*, vol. 300, no. 5623, pp. 1269–1272, 2003.

[11] K. Ueda, H. Tabata, and T. Kawai, "Ferromagnetism in $LaFeO_3$-$LaCrO_3$ superlattices," *Science*, vol. 280, no. 5366, pp. 1064–1066, 1998.

[12] H. Ohta, K. Nomura, M. Orita et al., "Single-crystalline films of the homologous series $InGaO_3(ZnO)_m$ grown by reactive solid-phase epitaxy," *Advanced Functional Materials*, vol. 13, no. 2, pp. 139–144, 2003.

[13] J. H. Kim, D. K. Seo, C. H. Ahn, S. W. Shin, H. H. Cho, and H. K. Cho, "Hybrid solution processed $InGaO_3(ZnO)_m$ thin films with periodic layered structures and thermoelectric properties," *Journal of Materials Chemistry*, vol. 22, no. 32, pp. 16312–16317, 2012.

[14] G. H. Kim, H. S. Shin, B. D. Ahn, K. H. Kim, W. J. Park, and H. J. Kim, "Formation mechanism of solution-processed nanocrystalline InGaZnO thin film as active channel layer in thin-film transistor," *Journal of the Electrochemical Society*, vol. 156, no. 1, pp. H7–H9, 2009.

[15] M. Ohyama, H. Kozuka, and T. Yoko, "Sol-gel preparation of ZnO films with extremely preferred orientation along (002) plane from zinc acetate solution," *Thin Solid Films*, vol. 306, no. 1, pp. 78–85, 1997.

[16] D. K. Seo, B. H. Kong, and H. K. Cho, "Composition controlled superlattice $InGaO_3(ZnO)_m$ thin films by thickness of ZnO buffer layers and thermal treatment," *Crystal Growth and Design*, vol. 10, no. 10, pp. 4638–4641, 2010.

[17] D. K. Seo, S. Shin, H. H. Cho, B. H. Kong, D. M. Whang, and H. K. Cho, "Drastic improvement of oxide thermoelectric performance using thermal and plasma treatments of the InGaZnO thin films grown by sputtering," *Acta Materialia*, vol. 59, no. 17, pp. 6743–6750, 2011.

[18] Z. X. Huang, Z. A. Tang, J. Yu, and S. Bai, "Thermal conductivity of nanoscale polycrystalline ZnO thin films," *Physica B*, vol. 406, no. 4, pp. 818–823, 2011.

[19] Y. Masuda, M. Ohta, W. S. Seo, W. Pitschke, and K. Koumoto, "Structure and thermoelectric transport properties of isoelectronically substituted $(Zno)_5In_2O_3$," *Journal of Solid State Chemistry*, vol. 150, no. 1, pp. 221–227, 2000.

[20] L. D. Zhao, Y. L. Pei, Y. Liu, D. Berardan, and N. Dragoe, "$InFeZnO_4$ as promising thermal barrier coatings," *Journal of the American Ceramic Society*, vol. 94, no. 6, pp. 1664–1666, 2011.